Factors Governing the Charge Density Wave Patterns of Layered Transition-Metal Compounds of Octahedral Coordination with d^2 and d^3 Electron Counts

Carme Rovira† and Myung-Hwan Whangbo*

Department of Chemistry, North Carolina State University, Raleigh, North Carolina 27695-8204

Received January 19, 1993®

Two different charge density wave (CDW) patterns are observed for layered transition-metal compounds ML_2 (e.g., M = transition metal, L = oxygen, chalcogen) of octahedral coordination with d^2 and d^3 electron counts. Tight-binding electronic band structure calculations were carried out for several d^2 ML_2 layers, and factors controlling these patterns were discussed. In general, the 1T-ML_2 systems with short M–L bonds adopt a CDW pattern involving a weak distortion, while those with long M–L bonds adopt a CDW pattern involving a strong distortion. Our calculations show that the metal-atom trimerization in $LiVO_2$ is energetically favorable and opens a band gap for a small displacement of the metal atoms. This supports the CDW model of weak metal-atom trimerization proposed for the $\sqrt{3} \times \sqrt{3}$ superstructure of $LiVO_2$.

Introduction

The CdI_2-type transition-metal compounds 1T-ML_2 (e.g., M = transition metal, L = chalcogen) consist of ML_2 layers made up of ML_6 octahedra (Figure 1a), and the metal atoms of an undistorted ML_2 layer form a hexagonal lattice (Figure 1b).[1] The ML_2 layers with d-electron counts d^1 to d^3 exhibit various patterns of metal-atom clustering, which are commonly referred to as charge density waves (CDW's).[2] The CDW pattern of zigzag chains (Figure 1c) is observed for the 1T-ML_2 layers containing d^2 ions, β-$MoTe_2$,[3] WTe_2,[3] α-ZrI_2,[4] and $M'Nb_2Se_4$ (M' = Ti, V, Cr).[5] In contrast, the d^2 1T-ML_2 systems 1T-MoS_2[6] and $LiVO_2$[7,8] do not exhibit a zigzag-chain clustering but a weak $\sqrt{3} \times \sqrt{3}$ superstructure. The $\sqrt{3} \times \sqrt{3}$ superstructure of $LiVO_2$ has been explained in terms of a weak trimerization of the metal atoms (Figure 1d) by Goodenough.[8] Different CDW patterns are also found for d^3 1T-ML^2 compounds: $ReSe_2$[9] and ReS_2[10] have a diamond-chain formation (Figure 1e), whereas ReO_2 has a zigzag-chain formation.[11] So far, the metal-atom trimerization model for the $\sqrt{3} \times \sqrt{3}$ superstructure has not been examined by electronic structure calculations, and factors controlling the CDW patterns of the 1T-ML_2 systems with a d^2 or d^3 electron count have not been well understood. In the present work, we probe these questions by performing extended Hückel tight-binding (EHTB) electronic band structure calculations[12,13] of several d^2 1T-ML_2 layers. A CDW is formed as a result of electron–phonon interactions. What kind of a CDW is likely to occur can be discussed on the basis of Fermi surface nesting.[14,15]

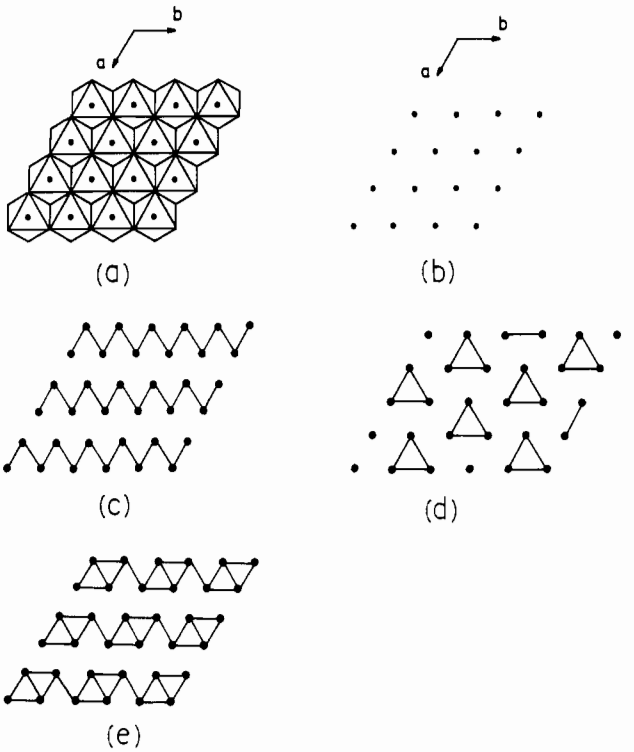

Figure 1. (a) Schematic projection view of an undistorted 1T-ML_2 layer along the direction perpendicular to the layer. (b) Metal ion arrangement in an undistorted 1T-ML_2 layer. (c) Zigzag-chain clustering of metal atoms in 1T-ML_2 with d^2 ions. (d) Trimerization of metal atoms in 1T-ML_2 with d^2 ions. (e) Diamond-chain clustering of metal atoms in 1T-ML_2 with d^3 ions.

† Permanent address: Departamento de Quimica Fisica, Universidad de Barcelona, 08028 Barcelona, Spain

® Abstract published in *Advance ACS Abstracts,* August 15, 1993.

(1) For early reviews, see: (a) Wilson, J. A.; Yoffe, A. D. *Adv. Phys.* **1969**, *18*, 193. (b) Hulliger, F. *Struct. Bonding* **1967**, *4*, 83.
(2) (a) Wilson, J. A.; DiSalvo, F. J.; Mahajan, S. *Phys. Rev. Lett.* **1974**, *32*, 882. (b) Wilson, J. A.; DiSalvo, F. J.; Mahajan, S. *Adv. Phys.* **1975**, *24*, 117. (c) Williams, P. M.; Parry, G. S.; Scruby, C. B. *Phil. Mag.* **1974**, *29*, 695. (d) Williams, P. M. In *Crystallography and Crystal Chemistry of Materials with Layered Structures*; Lévy, F., Ed.; Reidel: Dordrecht, The Netherlands, 1976; Vol. 2, p 51.
(3) Brown, B. E. *Acta Crystallogr.* **1966**, *20*, 268.
(4) Guthrie, D. H.; Corbett, J. D. *J. Solid State Chem.* **1981**, *37*, 256.
(5) Meerchaut, A.; Spiesser, M.; Rouxel, J.; Gorochov, O. *J. Solid State Chem.* **1980**, *31*, 31.
(6) Wypych, F.; Schöllhorn, R. *J. Chem. Soc., Chem. Commun.* **1992**, 1386.
(7) (a) Takei, H.; Koike, M.; Imai, K.; Sawa, H.; Kadowaki, H.; Iye, Y. *Mater. Res. Bull.* **1992**, *27*, 555. (b) Bongers, P. F. In *Crystal Structure and Chemical Bonding*; Rooymans, C. J. M., Rabenau, A., Eds.; Elsevier: New York, 1975; Chapter 4. (c) Kobayashi, K.; Kosuge, K.; Kachi, S. *Mater. Res. Bull.* **1969**, *4*, 95.
(8) (a) Goodenough, J. B.; Dutta, G.; Manthiram, A. *Phys. Rev. B* **1991**, *43*, 10170. (b) Goodenough, J. B. *Phys. Rev.* **1964**, *117*, 1442; **1960**, *120*, 67. (c) Goodenough, J. B. In *Magnetism and the Chemical Bond*; Wiley: New York, 1963; p 269.
(9) Alcock, N. W.; Kjekshus, A. *Acta Chem. Scand.* **1965**, *19*, 79.
(10) Wildervanck, J. C.; Jellinek, F. *J. Less-Common Met.* **1971**, *24*, 73.
(11) Magnéli, A. *Acta Chem. Scand.* **1957**, *11*, 28.
(12) Whangbo, M.-H.; Hoffmann, R. *J. Am. Chem. Soc.* **1978**, *100*, 6093.
(13) (a) Hoffmann, R. *J. Chem. Phys.* **1963**, *39*, 1397. (b) Ammeter, J. H.; Bürgi, H.-B.; Thibeault, J.; Hoffmann, R. *J. Am. Chem. Soc.* **1978**, *100*, 3686.
(14) Whangbo, M.-H.; Canadell, E. *J. Am. Chem. Soc.* **1992**, *114*, 9587.
(15) (a) Whangbo, M.-H.; Canadell, E.; Foury, P.; Pouget, J. P. *Science* **1991**, *252*, 96. (b) Canadell, E.; Whangbo, M.-H. *Chem. Rev.* **1991**, *91*, 965. (c) Whangbo, M.-H.; Ren, J.; Liang, W.; Canadell, E.; Pouget, J.-P.; Ravy, S.; Williams, J. M.; Beno, M. A. *Inorg. Chem.* **1992**, *31*, 4169.

0020-1669/93/1332-4094$04.00/0

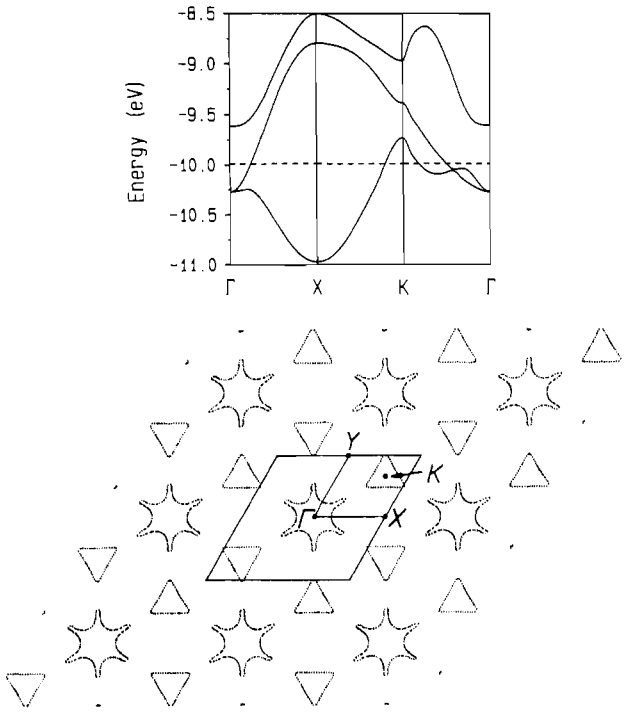

Figure 2. (a) Top: Dispersion relations of the t_{2g}-block bands calculated for a single VO_2^- layer of undistorted $LiVO_2$, where the dashed line is the Fermi level for the d^2 electron count. $\Gamma = (0, 0)$, $X = (a^*/2, 0)$, and $K = (a^*/3, b^*/3)$. (b) Bottom: Fermi surfaces associated with the partially filled t_{2g}-block bands of (a) in an extended zone, where $\Gamma = (0, 0)$, $X = (a^*/2, 0)$, $K = (a^*/3, b^*/3)$, and $Y = (0, b^*/2)$.

Hidden 1D bands of 1T-ML_2

The dispersion relations of the t_{2g}-block bands calculated for a single VO_2^- layer of the undistorted $LiVO_2$[7a] are shown in Figure 2a. For the d^2 electron count, these bands are partially filled and lead to the Fermi surfaces consisting of an electron pocket at Γ and a hole pocket at K (Figure 2b). Thus, $LiVO_2$ is predicted to be a two-dimensional (2D) metal, but it is a semiconductor below $T_p \approx 490$ K.[7,8] The latter has been interpreted to originate from a CDW of metal-atom trimerization (Figure 1d).[8] In general, the CDW phenomenon of a low-dimensional metal is explained in terms of the electronic instability associated with Fermi surface nesting. As already observed for the 1T type transition-metal dichalcogenides,[14] the Fermi surfaces calculated for undistorted 1T-ML_2 layers have a poor nesting and cannot be used to explain why the CDW instabilities arise.

The metal-atom clustering patterns in the 1T-ML_2 systems have been a subject of numerous theoretical studies.[14,16] The d-electron-count dependence of these patterns is explained on the basis of both local chemical bonding[14,16a] and hidden Fermi surface nesting[14,15] concepts. The ideal 1T-ML_2 layer of Figure 1a is decomposed into edge-sharing octahedral chains running along the a-, b-, or $(a + b)$-direction, as shown in Figure 3a-c. For convenience, the plane containing the shared edges of ML_6 octahedra is referred to as the equatorial plane, and the t_{2g} orbitals contained in the equatorial plane (see **1**) are referred to as the in-plane t_{2g} orbitals. Then, each ML_6 octahedron possesses three equatorial planes and three corresponding in-plane t_{2g} orbitals so that, given a set of edge-sharing octahedral chains parallel to the a-, b-, or $(a + b)$-direction, the metal–metal (M–M) interactions resulting from their in-plane t_{2g} orbitals are strong within each chain (being σ in nature) but weak between adjacent chains (being pseudo-δ in nature). On the basis of only the strong interactions between the in-plane t_{2g} orbitals, the t_{2g}-block bands of an undistorted 1T-ML_2 layer can be approximated as a superposition of the three independent one-dimensional (1D) bands (see Figure 4a) resulting from the three in-plane t_{2g} orbitals. These three 1D bands are termed the hidden 1D bands of an undistorted 1T-ML_2 layer.[14] The use of the hidden 1D surfaces is justified in discussing the CDW modulations of 1T-ML_2 systems, because the M–M interactions involving the in-plane t_{2g} orbitals contained in nonparallel equatorial planes become strongly weakened when structural modulations are introduced into the lattice.[14]

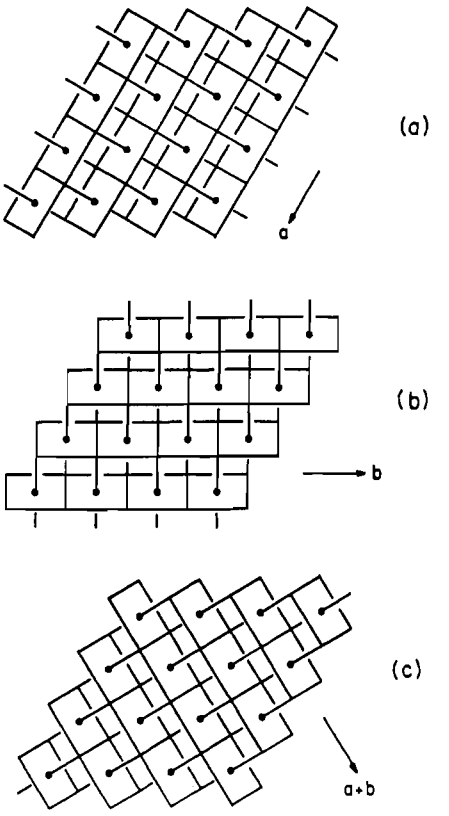

Figure 3. Decomposition of an undistorted 1T-ML_2 layer into sets of edge-sharing octahedral chains running along (a) the a-direction, (b) the b-direction, and (c) the $(a + b)$-direction.

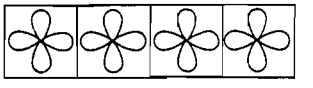

1

For the d^2 electron count, each hidden band becomes $^1/_3$-filled (Figure 4b), when the electrons are equally shared among the three bands. In general, a 1D band system with band occupancy $f = 1/n$ ($n = 2$, 3, etc.) is suspectible to a structural distortion that increases the unit cell size n times along the chain direction, for such a distortion introduces a band gap at the Fermi level and lowers the total energy.[14,15b] The three $^1/_3$-filled hidden 1D bands of Figure 4b predict a trimerization of the lattice along the a-, b- and $(a + b)$-directions. This prediction is consistent with the metal-atom trimerization model of Figure 1d, and hence with the $\sqrt{3} \times \sqrt{3}$ superstructure of 1T-MoS_2 and $LiVO_2$,[6-8] because every row of the metal atoms along the a-, b- or $(a + b)$-direction in Figure 1d has three metal atoms in a unit cell.

A d^3 1T-ML_2 system has three $^1/_2$-filled 1D bands (Figure 4c), which lead to diamond chains (Figure 1e) as a result of the dimerization associated with each $^1/_2$-filled band.[14] When two of the three 1D bands are filled with two electrons to become each $^1/_2$-filled (Figure 4d), zigzag chains are formed as a result of the associated dimerization in two directions [e.g., the a- and

(16) (a) Burdett, J. K.; Hughbanks, T. *Inorg. Chem.* **1985**, *24*, 1741. (b) Kertesz, M.; Hoffmann, R. *J. Am. Chem. Soc.* **1984**, *106*, 3453. (c) *Structure Phase Transitions in Layered Transition Metal Compounds*; Motizuki, K., Ed.; Reidel: Dordrecht, The Netherlands, 1986. (d) Doni, E.; Girlanda, R. In *Electronic Structure and Electronic Transitions in Layered Materials*; Grasso, V., Ed.; Reidel: Dordrecht, The Netherlands, 1986; p 1.

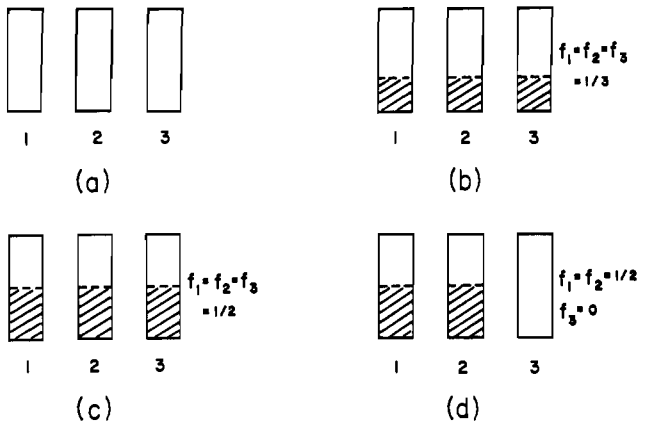

Figure 4. Schematic representations of the three hidden 1D bands comprising the t_{2g}-block bands of an undistorted 1T-ML_2 layer and their band occupancies: (a) Three hidden 1D bands; (b) three $^1/_3$-filled 1D bands expected for a d^2 1T-ML_2 system; (c) three $^1/_2$-filled 1D bands expected for a d^2 1T-MX_2 system; (d) two $^1/_2$-filled 1D bands and an empty band expected for a d^2 1T-ML_2 system.

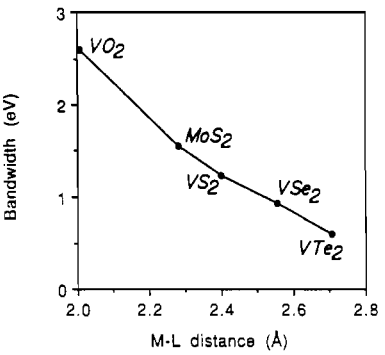

Figure 5. Widths of the t_{2g}-block bands calculated for the ideal 1T-ML_2 (ML_2 = VO_2, MoS_2, VS_2, VSe_2, VTe_2) layers constructed from regular ML_6 octahedra.

(a + b)-directions in Figure 1c].[14] For a d^2 1T-ML_2 system, therefore, the zigzag chain formation arises from the disproportionate band filling (Figure 4d), and the $\sqrt{3} \times \sqrt{}$ superstructure from the proportionate band filling (Figure 4b).

Factors Influencing the CDW Patterns of d^2 or d^3 1T-ML_2

The CDW pattern of a d^2 1T-ML_2 system should be determined by the balance of several competing energy factors, e.g., the energy required for the disproportionate band filling, the enhancement of the M–M bonding interaction by the metal-atom clustering, and the lattice strain resulting from the metal-atom clustering. Let us consider "ideal" 1T-ML_2 layers made up of regular ML_6 octahedra. Then, with decreasing of the metal–ligand (M-L) bond length, the M–M distance becomes smaller so that the M–M interaction becomes stronger, and the M–L bond becomes less polarizable so that the lattice strain increases. Note that the zigzag chain formation is found for the d^2 1T-ML_2 systems with a long M–L bond [i.e., $MoTe_2$, WTe_2, and $M'Nb_2Se_4$ (M' = Ti, V, Cr)] and not for those with a short M–L bond (i.e., $LiVO_2$ and 1T-MoS_2).

The zigzag chain formation arises from the disproportionate band filling of Figure 4d. The latter requires an electron transfer from one of the t_{2g}-block bands to the remaining two (Figure 4d vs Figure 4b); i.e., a "promotion energy" is needed. This energy increases, and hence the zigzag chain formation becomes less favorable, with increasing the width of the hidden 1D bands (or, equivalently, that of the t_{2g}-block bands). As shown in Figure 5, which summarizes our EHTB calculations for the "ideal" 1T-ML_2 layers (ML_2 = VO_2, MoS_2, VS_2, VSe_2, VTe_2), the width of the "ideal" t_{2g}-block bands becomes gradually narrower with increasing the M–L distance. (The atomic parameters used for our EHTB calculations are summarized in Table I. The M–L bond lengths used to construct the ML_6 octahedra are V–O = 2.007 Å, Mo–S = 2.285 Å, V–S = 2.400 Å, V–Se = 2.557 Å, and V–Te = 2.709 Å.[17]) According to Figure 5, the ideal 1T-ML_2 layers will have a larger t_{2g}-block bandwidth for $LiVO_2$ and 1T-MoS_2 compared with the other d^2 1T-ML_2 systems exhibiting the zigzag-chain formation. This is consistent with the finding that the zigzag-chain formation is unfavorable in $LiVO_2$ and 1T-MoS_2.

Table I. Exponents ζ_i and Valence Shell Ionization Potentials H_{ii} of the Slater Type Orbitals χ_i Used in the EHTB Calculations[a]

atom	χ_i	H_{ii} (eV)	ζ_i	c_1[b]	ζ'_i	c_2[b]
V	4s	−8.81	1.30			
	4p	−5.52	1.30			
	3d	−11.00	4.75	0.4755	1.70	0.7052
Mo	5s	−8.34	1.96			
	5p	−5.24	1.90			
	4d	−10.50	4.54	0.5899	1.90	0.5899
O	2s	−32.3	2.275			
	2p	−14.8	2.275			
S	3s	−20.00	1.817			
	3p	−13.30	1.817			
Se	4s	−20.50	2.44			
	4p	−13.20	2.07			
Te	5s	−20.78	2.51			
	5p	−13.20	2.16			

[a] H_{ii}'s are the diagonal matrix elements $\langle\chi_i|H^{eff}|\chi_i\rangle$, where H^{eff} is the effective Hamiltonian. In our calculations of the off-diagonal matrix elements $H_{ij} = \langle\chi_i|H^{eff}|\chi_j\rangle$, the weighted formula was used.[13b] [b] Contraction coefficients used in the double-ζ Slater type orbital.

The M–M and M–L distances are shorter, and thus the lattice strain should be larger, in the 1T-VO_2- and 1T-MoS_2 layers than in the other d_2 1T-ML_2 layers. Therefore, the stabilization energy resulting from the metal-atom trimerization (Figure 1d) should be substantial for a small displacement of the metal atoms in $LiVO_2$ and 1T-MoS_2. As a representative example, we calculate how the band electronic structure of a single 1T-VO_2^- layer is affected as the metal-atom trimerization progresses. For simplicity, we define the extent of the trimerization in terms of the metal atom displacement δ shown in **2**. As δ increases, the

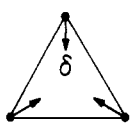

2

equilateral triangle of each metal trimer becomes smaller without moving the oxygen atoms of the lattice. Figure 6a presents the band gap E_g of a single 1T-VO_2-layer as a function of δ, and Figure 6b the stabilization energy ΔE of a single 1T-VO_2^- layer as a function of δ. As anticipated, the E_g and ΔE values are sensitive to the displacement δ. The band gap opening occurs for a very small value of δ ($\geq$0.023 Å), and the total electronic energy is gradually lowered with increasing δ. Due the lattice strain, which increases with δ, the total energy of the lattice should be raised beyond a certain δ value. Experimentally, the band gap E_g for single-crystal samples of $LiVO_2$ is estimated to be 0.1–0.2 eV.[7a] According to our calculations, this range of E_g occurs for the very small displacement δ = 0.026–0.030 Å (Figure 6a), for which the lattice is stabilized by 12–16 kcal/mol per $(VO_2^-)_3$ unit (Figure 6b). Thus, the CDW model of weak metal-atom trimerization proposed by Goodenough[8] for the $\sqrt{3} \times \sqrt{3}$ superstructure of $LiVO_2$ is fully supported by the present study. This model should also be appropriate for 1T-MoS_2.

(17) These M–L bond lengths were obtained as follows: V–O = V–V/$\sqrt{2}$ with V–V = 2.839 Å;[7] Mo–S = Mo–Mo/$\sqrt{2}$ with Mo–Mo = 3.231 Å;[6] V–S is the average of the V–S bond lengths in $VS_{1.47}$;[22] V–Se is the average of the V–Se bond lengths in V_3Se_4;[23] V–Te is the average of the V–Te bond lengths in 1T-VTe_2.[24]

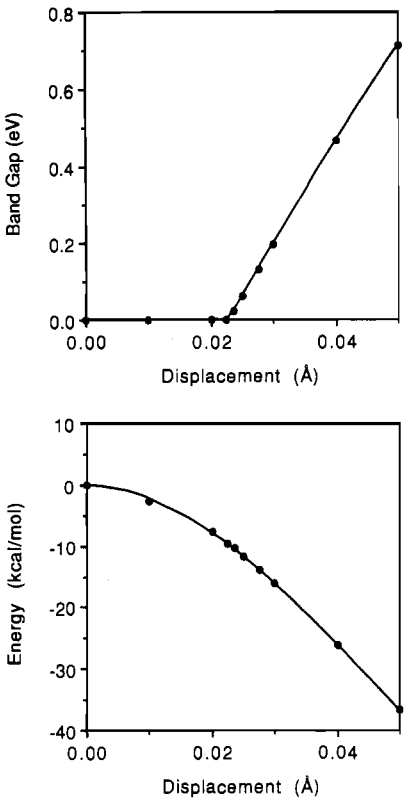

Figure 6. (a) Top: Band gap E_g (eV) of a single 1T-VO_2 layer as a function of the metal-atom displacement δ (Å). (b) Bottom: Stabilization energy ΔE, in kcal/mol per $(VO_2^-)_3$, of a single 1T-VO_2 layer as a function of the metal-atom displacement δ (Å).

For ideal d^2 1T-ML_2 systems with long M–L bonds, a small M–M shortening cannot provide a significant energy lowering because the M–M distance is not short enough to provide a strong M–M bonding. From the viewpoint of local chemical bonding, the zigzag chains result when each metal atom makes two two-center two-electron σ-bonds with its neighboring metal atoms by utilizing the in-plane t_{2g} orbitals.[14,16a] The formation of such M–M σ-bonds requires a large lattice distortion in the d^2 1T-ML_2 layers with long M–L bonds. A long M–L bond is polarizable, so that the M–M σ-bond formation may not induce a strong lattice strain. In addition, an ideal 1T-ML_2 lattice with a long M–L bond will have a narrow t_{2g}-block bandwidth and hence a small promotion energy for the disporportionate band filling. Consequently, the zigzag-chain formation is favorable for the d^2 1T-ML_2 systems with long M–L bonds.

At room temperature ReO_2 exhibits zigzag chains instead of diamond chains, although it contains d^3 metal ions as do $ReSe_2$ and ReS_2. A diamond chain is a dimerized form of a zigzag chain,[18] so that a diamond-chain formation induces a greater lattice strain than does a zigzag-chain formation. The Re–O distance is shorter than the Re–S or Re–Se distance, so that the lattice strain is greater in the ReO_2 layer than in the $ReSe_2$ and ReS_2 layers. Thus, it is speculated that the lattice strain is too strong for ReO_2 to form diamond chains. (It is worthwhile to note that $Na_3Cu_4S_4$ is a 1D metal[19] but does not exhibit any CDW instability down to 13 K.[20] The lattice vibration needed for a CDW formation probably induces a severe lattice strain.[19]) For the d^3 electron count, a 1T-ML_2 layer with zigzag chains has partially filled t_{2g}-block bands[18] so that ReO_2 is predicted to be a 1D metal. It would be interesting to examine whether or not CDW fluctuations[21] occur in ReO_2 as the temperature is lowered.

Concluding Remarks

Two different CDW patterns are observed for d^2 or d^3 1T-ML_2 systems depending on the nature of the metal M and the ligand L. Which CDW pattern is favored by a given system depends on several competing energy terms associated with the CDW formation. Two crucial factors are the M–M bonding interaction and the lattice strain, both of which are intimately related to the M–L bond length. In general, the 1T-ML_2 systems with short M–L bonds prefer a CDW pattern involving a small metal-atom displacement, while those with long M–L bonds prefers a CDW pattern involving a large metal-atom displacement. Our electronic band structure calculations show that the metal-atom trimerization in $LiVO_2$ lowers the total energy and opens a band gap for a very small displacement of the metal atoms, thereby supporting the CDW model of weak metal-atom trimerization proposed for the $\sqrt{3} \times \sqrt{3}$ superstructure of $LiVO_2$. This model is also appropriate for the $\sqrt{3} \times \sqrt{3}$ superstructure of 1T-MoS_2.

Acknowledgment. This work was supported by the U.S. Department of Energy, Office of Basic Sciences, Division of Materials Sciences, under Grant DE-FG05-86ER45259. We thank Dr. E. Canadell for an invaluable discussion and a reference.

(18) Canadell, E.; LeBeuze, A.; El Khalifa, M. A.; Chevrel, R.; Whangbo, M.-H. *J. Am. Chem. Soc.* **1989**, *111*, 3778.
(19) Whangbo, M.-H.; Canadell, E. *Inorg. Chem.* **1990**, *29*, 1395.
(20) Peplinski, Z.; Brown, D. B.; Watt, T.; Hatfield, W. E.; Day, P. *Inorg. Chem.* **1982**, *21*, 1752.
(21) Moret, R.; Pouget, J. P. In *Crystal Chemistry and Properties of Materials with Quasi-One-Dimensional Structures*; Rouxel, J., Ed.; Reidel: Dordrecht, The Netherlands, 1986; p 87.
(22) Kawada, I.; Nakano-Onoda, M.; Ishi, M.; Saeki, M.; Nakahira, M. *J. Solid State Chem.* **1965**, *15*, 246.
(23) Kallel, A.; Boller, H. *J. Less-Common Met.* **1984**, *102*, 213.
(24) Bronsema, K. D.; Bus, G. W.; Wiegers, G. A. *J. Solid State Chem.* **1984**, *53*, 415.